1   ***Formulation of a composite nasal spray enabling enhanced surface coverage and***

2   ***prophylaxis of SARS-COV-2***

3   R. J. A. Moakes[1*], S. P. Davies[2], Z. Stamataki[2], L. M. Grover[1*]

4   [1] Healthcare Technology Institute, School of Chemical Engineering, University of Birmingham, Birmingham,

5   UK

6   [2] Institute of Immunology and Immunotherapy, School of Medicine and Dentistry, University of Birmingham,

7   Birmingham, UK

8

9   Corresponding authors (*): r.j.a.moakes@bham.ac.uk; l.m.grover@bham.ac.uk

10   ***Abstract***

11   Airborne pathogens pose high risks in terms of both contraction and transmission within the

12   respiratory pathways, in particular the nasal region. Although knowledge of airborne

13   transmission has long been known, there is little in the way of adequate intervention that can

14   protect the individual, or even prevent further spread. This study focuses on a nasal applicant

15   with the capacity to combat such issues, by focussing on the SARS-CoV-2 virus. Formulation

16   of a spray containing polysaccharides known for their mucoadhesive properties was

17   undertaken and characterised for their mechanical, spray patterns and antiviral properties.

18   The ability to engineer key behaviours such as yielding have been shown, through systematic

19   understanding of a composite mixture containing two polymers: gellan and λcarrageenan.

20   Furthermore, spray systems demonstrated highly potent antiviral capacities, resulting in

21   complete inhibition of the virus when studied for both prophylaxis and prevention of spread.

22   Finally, a mechanism has been proposed to explain such findings. Therefore, demonstrating

23   the first fully preventative device, targeted to protect the lining of the upper respiratory

24   pathways.

25   ***Key words***

26   COVID/SARS-CoV-2/Prophylaxis/Nasal Spray/Formulation/Polysaccharides/Carrageenan

27   ***Introduction***

28   Transmission of viruses occurs through 4 routes: direct contact, via physical contact with a

29   carrier; indirect contact, interactions with contaminated objects; droplet and airborne

30   transmission, often through coughs, sneezes and breathing; and, aerosolization, atomised

31   virus suspended in airflow.[1] Airborne transmission of respiratory pathogens, whether

32   through droplets or atomisation, is particularly deleterious, with the virus effectively and

33   locally delivered to the respiratory pathways. Recent work, primarily undertaken within the

34   COVID-19 pandemic has heavily focused on providing a deeper understanding on person to

35   person airborne transmission.[2–5] During the act of coughing, turbulent air forces mucus

36   breakup into droplets[6] (*ca*. 0.62 to 15.9 μm),[7] which are then expelled through the oronasal

37   passages at flow rates of up to 12 Ls^{-1}, reaching velocities of up to 30 ms^{-1}.[8] Unfortunately,

38   the expelled cloud is subject to many varying parameters: speed of expulsion, droplet size

39   and environmental effects such as air speed, resulting in effected boundaries ranging from *ca*.

40   0.5 to 8 m.[8,9] It is likely, for this reason, that the inability to standardise transmission in this

41   way has led to an ongoing lack of change in regard to the concepts employed to cope with

42   such issues;[10] with recommended distancing guidelines still based on the ideas portrayed by

43   Chaplin and Wells close to a century ago.[11,12] Although the epidemiology of the severe acute

44   respiratory syndrome coronavirus 2 (SARS-CoV-2) is not yet definitive, clear indications

45   suggest epidemiological characteristics closely linked to airborne transmittance[13].

46

47   There are many airborne viruses including: influenza-, rhino-, adreno-, entero- and corona-

48   virus. The latter, *coronaviridae* (CoVs) family, are implicated in a variety of gastrointestinal,

49   central nervous system and respiratory diseases (MERS, SARS);[14] with the latest strain,

50   SARS-CoV-2, receiving much attention due to its devastating impact within the 2020

51   pandemic. SARS-CoV-2, like all coronaviruses, contains large positive-strand RNA genomes

52   packed within a helical capsid, all housed within a phospholipid bilayer envelope formed on

53   budding.[15,16] Associated with the viral membrane are 3 main proteins: membrane and

54   envelope proteins, associated with assembly, and spike proteins. The spike proteins, which

55   give rise to its corona shape, are essential for virus survival, mediating entry to the host

56   cell.[17,18] Additionally, the protein also plays a crucial role in determining host range and

57   tissue tropism, alongside being responsible for inducing many of the host immune

58   responses.[14] To date, facilitation of viral entry into a host cell is believed to arise through

59   specific motifs within the spike protein, which strongly interact with Angiotensin-Converting

60   Enzyme 2 (ACE2) receptors.[19,20] ACE2 is known for its role in regulating oxygen/carbon

61   dioxide transfer, commonly found within the respiratory epithelia. In particular SARS-CoV-2

62   has been found to target the ciliated and goblet cells,[21] where subsequent viral shedding

63   results in extensive viral loads, especially within the upper respiratory tract.[22]

64

65   Respired air is primarily routed through the nose. Even though the nasal passages present the

66   highest resistance to airflow, on average *ca*. 10,000 L of air is inhaled by a healthy human per

67   day.[23,24] Only once this pathway becomes overloaded does the body switch to respiratory

68   through the mouth.[25][26] For this reason, the nasal cavity supports two major roles: climate

69   control, creating the correct levels of humidity and air temperature; and, removal of foreign

70   particles including dust, airborne droplets and pathogens.[27] Anatomically, the nose consists

71   of 2 cavities roughly 10 cm in length and half again in height, producing a total surface area

72   of about 150 cm^2.[28] Inspired air flows up through the nasal vestibule (nostril) and passes

73   through the slit-like meatus structures (inferior, middle and superior) and back through the

74   nasopharynx. At a cellular level the majority of the cavity consists of a typical airway

75   epithelium, comprising of 4 main cell types: basal, ciliated/non-ciliated columnar and goblet

76   cells. The columnar cells, whether ciliated or not, are coated by microvilli. Their role, to

77   prevent drying, supports the cilia in performing mucociliary clearance of mucins produced in

78   the goblet cells.[29,30] Additionally, the presence of cilia and microvilli drastically increases the

79   effective surface area (*ca*. 9.6 m^2), providing a highly efficient platform for filtration.[31]

80   Unfortunately, such large surface areas also provides greater exposure in terms of viral entry.

81

82   The airborne risk imposed not only through ventilation systems and crowds, but re-

83   suspension of the virus from inanimate objects, including personal protective equipment,[32]

84   vociferates the need for new and novel devices that not only prevent contraction, but stop

85   spread thereafter. This study looks to address such issues, by specifically engineering spray

86   formulations which target the nasal passages. The emphasis on speed within such

87   unprecedented times in terms of translating the fundamental science from lab to clinic, drives

88   key considerations such as simplicity and proven biocompatibility. As such, colloidal

89   composites of FDA approved polymers were studied for their application as nasal sprays.

90   Systems were deconstructed back to their single constituents, and characterised for their

91   mechanical, spray and antiviral properties. As such a set of design principles was determined

92   in order to present a potential nasal spray to combat airborne pathogens, in particular SARS-

93   CoV-2.

94   ***Results***

95   *Physico-mechanical behaviours of the nasal spray formulation*

96   On application, nasal sprays directly contact the nasal mucosa lining the epithelium (Fig. 1a).

97   Longevity of the applicant can be improved via careful choice of the polymer, promoting

4

98   interaction with the mucus; known as mucoadhesion. A range of polymers known for their

99   mucoadhesive properties (gellan, carrageenan, alginate, pectin, dextran) were screened

100   through spray application to a 45° acetate surface (Fig. 1b). Polymers were classed for their

101   ability to create an even coverage whilst being retained at the sprayed site. Fig. 1bii and 1biii

102   shows typical images for several of the polymers tested, demonstrating a "good" and "poor"

103   candidate; gellan and alginate respectively. Screening in this manner provided a means to

104   narrow the systems down to both gellan and carrageenan going forward, with others either

105   creating heterogeneous distributions or flowing under their own mass.

106

107   Flow behaviours were characterised via dynamic viscosity (from high to low shear stress),

108   representative of the material once sprayed. Resultant profiles for the gellan were modelled

109   demonstrating a transition from power law to Cross model, suggesting the loss of a dynamic

110   yield stress to zero-shear viscosity as a function of the polymer concentration (Fig. 1ci). No

111   transition was observed for the λcarrageenan systems, characterised solely by the Cross

112   model at all polymer concentrations studied (Fig. 1cii). Zero-shear viscosity was dependent

113   on polymer content, providing viscosities within the range of 0.27 to 0.01 mPa.s for 1.0 to
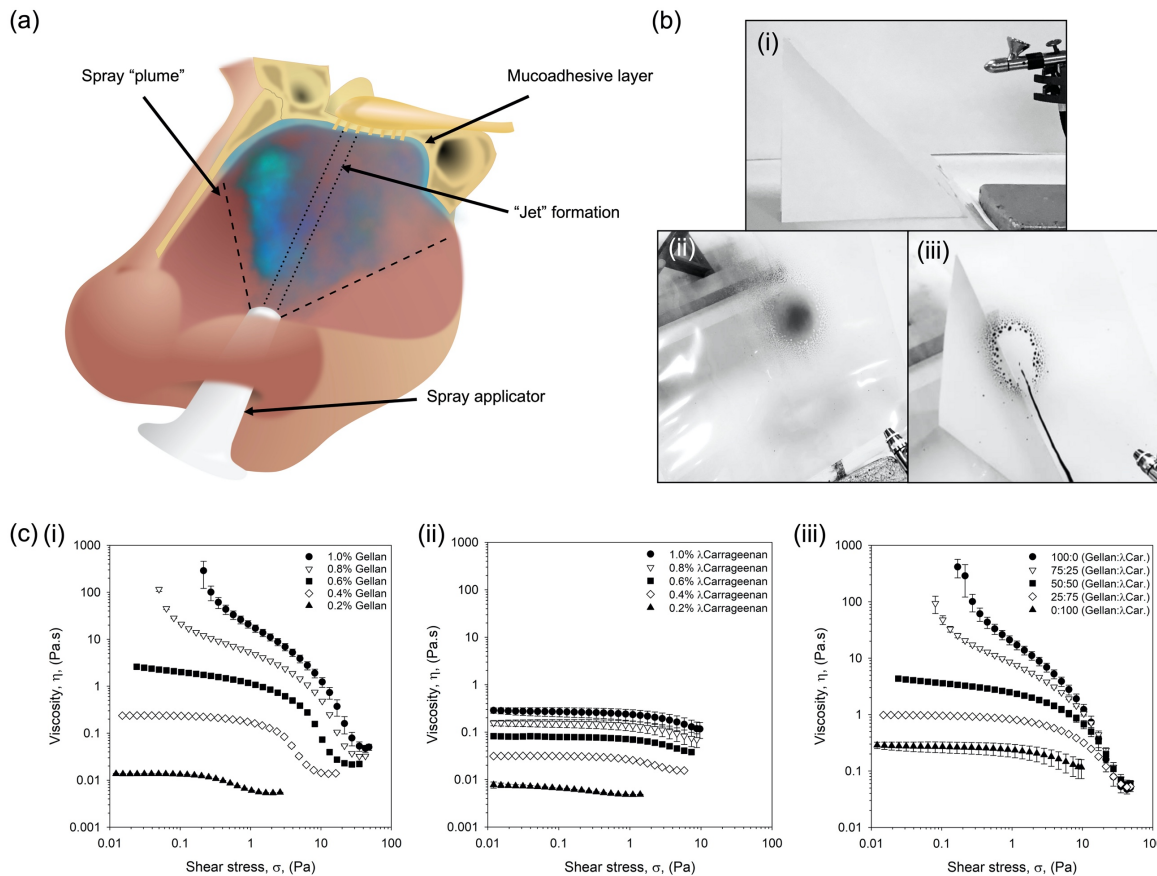
114   0.2% (w/v), respectively.

115

*Figure 1: **Defined nasal spray behaviours.** (a) Schematic diagram demonstrating the application of a nasal spray to the nasal cavity. (b) Typical images obtained during screening of numerous mucoadhesive polymers for their ability to evenly spray and be retained on a 45° incline: (i) spray set up, (ii) gellan gum 1% (w/v) with black dye, and (iii) alginate 1% (w/v) with black dye. (c) Dynamic viscosity profiles from high to low shear stress for: (i) gellan samples with concentrations ranging from 0.2 to 1.0% (w/v), (ii) λcarrageenan samples with concentrations ranging from 0.2 to 1.0% (w/v), and (iii) composite systems of gellan:λcarrageenan at a total polymer concentration of 1% (w/v).*

Viscosity curves for the composite mixtures containing both the gellan and the λcarrageenan (ratios of 100:0, 75:25, 50:50, 25:75 and 0:100) have been shown in Fig. 1ciii and Table 1. Flow behaviours for the 1% (w/v) systems showed a clear transition from material characteristics indicative of the gellan (viscosity asymptoting at low stresses), to those of the λcarrageenan (plateaued viscosities at low stresses), as the ratio of the two polymers shifted from one extreme to the other (gellan to λcarrageenan). Loss of overall viscosity was also observed as the systems shifted from high to low gellan ratios, confirmed by the reduction in consistency coefficient (K) from 3.54 to 0.03. This correlated well with the increase in rate

6

132   index (n), where more gellan resulted in higher degrees of shear thinning: 0.40 to 0.82 for

133   100% gellan and 100% λcarrageenan, respectively. A reduction in the total polymer content

134   to 0.4% (w/v) resulted in all mixtures characterised by the Cross model, consistent with data

135   provided for the isolated polymers. Further reduction in the polymer concentration, to 0.2%

136   (w/v), resulted in profiles independent on the ratio of gellan to λcarrageenan, with samples

137   indistinguishable from each other (within error).

138   *Table 1: **Comparison of viscometry data.** Tabulated viscometry data compiled for composite systems modelled either using*
139   *the power law model (no zero-shear data provided) or Cross model (zero-shear data).*

Total Polymer (% (w/v))	Polymer Ratio (Gellan:λCar.)	Zero-Shear Viscosity (Pa.s)	Consistency Coefficient (K)	Rate Index (n)
1.0	*100:0*	N/a	3.544±**0.319**	0.403±**0.004**
	75:25	N/a	2.693±**0.075**	0.491±**0.002**
	50:50	4.080±**0.324**	1.163±**0.034**	0.543±**0.005**
	25:75	0.988±**0.013**	0.094±**0.002**	0.727±**0.012**
	0:100	0.274±**0.046**	0.030±**0.009**	0.821±**0.151**
0.4	*100:0*	0.245±**0.002**	0.065±**0.004**	0.831±**0.003**
	75:25	0.172±**0.005**	0.060±**0.001**	0.692±**0.054**
	50:50	0.083±**0.000**	0.020±**0.002**	1.021±**0.084**
	25:75	0.052±**0.002**	0.016±**0.000**	1.134±**0.029**
	0:100	0.032±**0.001**	0.013±**0.001**	1.293±**0.051**
0.2	*100:0*	0.014±**0.000**	0.021±**0.000**	1.315±**0.161**
	75:25	0.009±**0.000**	0.022±**0.000**	1.413±**0.025**
	50:50	0.010±**0.000**	0.017±**0.003**	1.341±**0.287**
	25:75	0.007±**0.000**	0.016±**0.007**	1.283±**0.403**
	0:100	0.007±**0.000**	0.026±**0.001**	1.288±**0.056**

140

141   Viscometry data was used to better understand the potential residence of the spray within the

142   nasal cavity. As such, Eq. 1 was used to predict the stress exerted on the material under

143   gravity residing on an incline.

144

145                              $\sigma_{max} = \rho.g.h.(sin\theta)$ [1]

7

146

147   Where ρ is the density of the nasal spray (kg.m^{-3}), g is the force due to gravity (9.807 m.s^{-2}), h

148   is the thickness of the sprayed layer (m) and θ is the inclined angle. Applying values for the

149   polymer suspensions based on a maximum 500 μm thick sprayed layer at 45° (Eq. 2) resulted

150   in a theoretical stress of 7 mPa.

151

152 $$\sigma_{max} = 1.01 \times 9.807 \times 1x10^{-3}(\sin 45) \qquad [2]$$

153

154   A simple force balance revealed insufficient stress under gravity to induce flow in any of the

155   systems containing a dynamic yield stress. Indeed, even in systems described by the Cross

156   model, the external stress due to gravity was not sufficient to move the system from its zero-

157   shear plateau into the thinning region.

158   *Understanding formulation spray-ability*

159   Application of the polymeric materials through a typical hand spray aperture has been shown

160   in Fig. 2. Spray distributions for the single polymer systems have been demonstrated in Fig.

161   2a. Gellan demonstrated an inherent ability to spray forming a typical "plume" across all

162   concentrations studied. In contrast, even at the lowest concentration, λcarrageenan systems

163   demonstrated a degree of "jetting", becoming more visible as the polymer concentration

164   increased. Aspirate formation on leaving the nozzle was reflected in the distributions formed

165   on contact with the substrate (Fig. 2b). Here, following increasing polymer, distributions

166   became narrower with fewer satellite droplets forming around the central accumulation. A

167   general negative correlation between %coverage and total polymer concentration was drawn,

168   loosely fitting a linear trend (R^2 = 0.72 and 0.62 for both gellan and λcarrageenan,

169   respectively) (Fig. 2ci). Furthermore, it was observed that all gellan concentrations resulted in

170   higher coverage than the λcarrageenan, demonstrating maximum and minimum %coverage

171   of 28.5-20.7% when compared to 15.9-6.1% for the λcarrageenan systems (0.2 and 1.0%
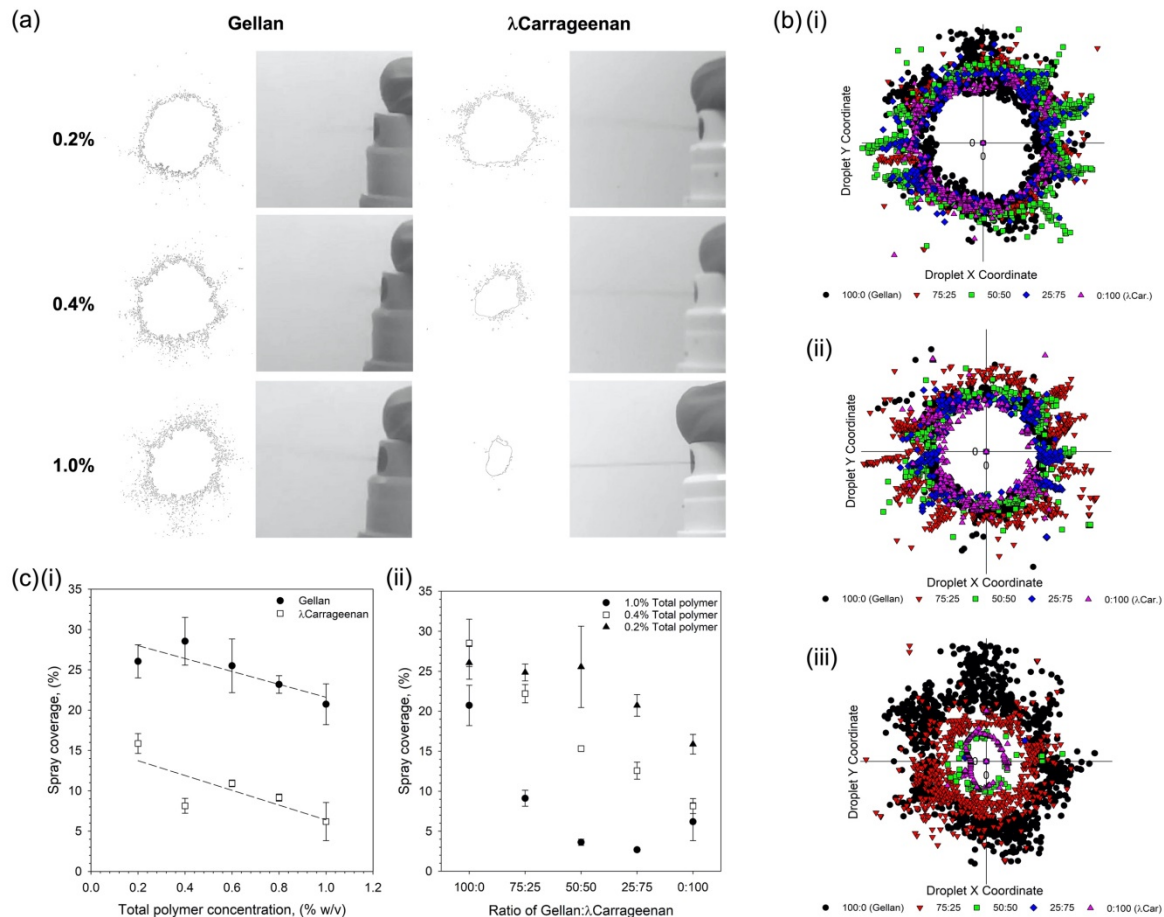
172   (w/v) polymer, respectively).

173

*Figure 2: **Spray-ability of polymer suspensions.** (a) typical images of the spray formation as the polymer suspensions are*
aspirated form the applicator, alongside resulting distribution outlines for a range of polymer concentrations. (b) overlay of
droplet distributions from a central point showing the reduction in spray as a function of the ratio of gellan to λcarrageenan
for: (i) 0.2% (w/v) total polymer, (ii) 0.4% (w/v) total polymer, and (iii) 1% (w/v) total polymer. (c) spray coverage as
determined using an imaging software for: (i) single polymer suspensions (trend lines are denoted by the dashed line with
$R2$ values of 0.72 and 0.62 for the gellan and λcarrageenan, respectively), and (ii) composite mixtures of the gellan and
λcarrageenan at either 0.2, 0.4 or 1.0% (w/v) total polymer.

181   The role that total and ratio of polymer play within the spray-ability of the composite systems

182   can be clearly seen in Fig. 2b. In all instances, irrespective of total polymer concentration, a

183   shift to smaller distributions was observed as the ratio of gellan to λcarrageen decreased.

184   Such changes became more pronounced with total polymer, where the magnitude of change

9

185 between 100% gellan to 100% λcarrageenan, followed 1.0%> 0.4%> 0.2% (w/v). such

186 observations were mirrored in the total coverage data (Fig. 2cii). Replacing 25% of the total

187 λcarrageenan with gellan resulted in a 4.9% and 4.4% increase in coverage, for the 0.2% and

188 0.4% (w/v) systems; with an initial loss in spray coverage (-3.5%) for the 1% total polymer

189 content. Coverage was further increased to 9.0%, 14.1% and 2.9% for the 0.2, 0.4 and 1.0%

190 (w/v) systems respectively at a ratio of 75:25 (gellan:λcarrageenan).

191 *In vitro analysis of the nasal spray formulations*

192 First hit and transmission of the virus was studied *in vitro* using SARS-CoV-2 infection of

193 Vero cells. An initial study was undertaken to determine cell compliance with the sprays over

194 a 48 hrs incubation period (Fig. 3ai). Cell tolerance was dependent on the polymer

195 concentration, demonstrating a 2-fold reduction in the number of living cells for both the

196 gellan and the λcarrageenan at a dilution of 1/2. Dose-response of cell viability was linear (R^2

197 = 0.96 and 0.97 for gellan and λcarrageenan, respectively), with reduced cell death as the

198 systems became increasing more dilute.

199

200 Prevention of both contraction and/or transmission of the virus was assessed by two treatment

201 regimens: treating the virus with the compound prior to infecting the cells (referred to as

202 virus treated); or, by first treating the cells before introduction of the virus (referred to as cells

203 treated). Fig. 3aii and aiii show the effect of the single polymer systems on resultant infection

204 when treated with the virus- and cell-first regimens, respectively. It was observed that in the

205 case of the gellan only, all dilutions resulted in infection irrespective of treatment regime

206 after 24 hrs. Indeed after 48 hrs, such observations were exacerbated with dilutions greater

207 than 1/3 resulting in levels of infection above the control. Interestingly, the λcarrageenan

208   treated systems showed no signs of infection above the uninfected control at either time

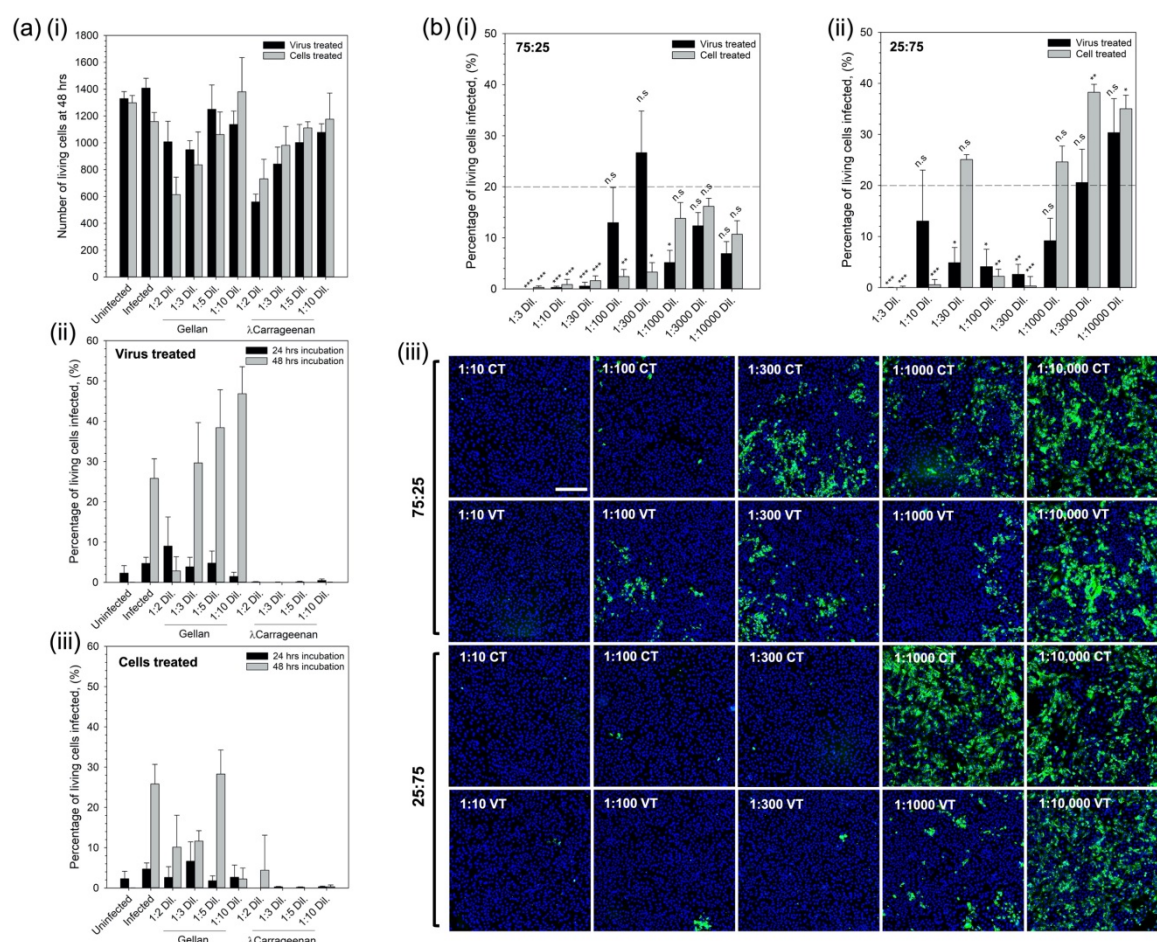209   point, 24 or 48 hrs, irrespective of the treatment regimen.

211   *Figure 3: **First hit and transmission analysis prevention.** In vitro SARS-CoV-2 assay using vero cells to determine (a)(i)*
212   *cell tolerance to the nasal sprays (live/dead analysis), (ii) degree of infection at 24 and 48 hrs for cells inoculated with the*
213   *virus having undergone a pre-treatment with either the gellan or λcarrageenan spray, and (iii) degree of infection at 24 and*
214   *48 hrs for spray-treated cells inoculated with the virus. (b) degree of infection for the composite mixtures (1% (w/v) total*
215   *polymer) after 48 hrs incubation having undergone either the virus treated or cell treated regimens for, (i) 75:25% gellan to*
216   *λcarrageenan, or (ii) 25:75% gellan to λcarrageenan, systems, and (iii) typical fluorescent micrographs of treated systems*
217   *using Hoechst staining, scale bar shows 200 μm (blue denotes non-infected and green infected cells). (n.s – not statistically*
218   *different, * - p<0.05, ** - p<0.01, and *** - p<0.001)*

219   Composite systems containing 1% total polymer at either a ratio of 75:25 or 25:75 (gellan to

220   λcarrageenan) were also studied using the same treatment regimens over 48 hrs; data

221   presented in Fig. 3b. Composites of a ratio 75:25 showed significant suppression of the

222   infection (minimum of p<0.05) up to a dilution of 1/000 on comparison with the untreated

223   control group (Fig. 3bi). In contrast, composites at a ratio of 25:75 comprising a higher

11

224 proportion of λcarrageenan, demonstrated fluctuations in suppression with dilutions of 1/30,

225 1/1000, 1/3000 and 1/10000 all resulting in infection levels equal to or greater than the

226 untreated control (Fig. 3bii). Comparison of the treatment regimens highlighted key

227 differences in the ability to supress infection. Again, for the 25:75 composite it can be seen

228 that at lower dilution factors, between 1/3 and 1/300 (with the exception of 1/30), resulted in

229 lower average responses for cells treated prior to infection when compared to treating the

230 virus first. However, at larger dilution factors (>1/300) it became apparent that treatment of

231 the virus first becomes more effective. This can be seen more clearly in the images showing

232 Hoechst stained cells, where the extent of infected cells (green – spike 2 protein staining) was

233 much less for the virus treated groups when compared to the cell treated groups.

234 *Spray mechanism of inhibition*

235 Polymer chemistry was studied in relation to the polymer type and degree of sulphation in

236 order to better understand the mechanism of infection inhibition. Initial experiments were

237 conducted to ascertain adherence of the polymer to the cell membrane. Staining (Alcian blue)

238 of the sugar chains was conducted post treatment and washing. Fig. 4b shows staining

239 intensity as a function of: polymer type, gellan and carrageenan; and, degree of sulphation

240 along the carrageenan backbone, ι and λ. Intensity data highlighted a significant difference

241 (p<0.001) between cells treated with a 1/3 dilution of both carrageenans when compared to

242 the cells only group. Moreover, when compared to the stained cells only group, significance

243 remained (p<0.01). Inter-carrageenan analysis demonstrated ιcarrageenan to had a higher

244 average intensity in comparison to the λcarrageenan (56.2% and 44.4%, respectively). To

245 determine whether the degree of sulphation across the polymer backbone was important in

246 suppression of the infection, κ–, ι– and λ–carrageenan were studied using the SARS-CoV-2

247 assay (Fig. 4c). It was observed that in all cases, where the cells were treated prior to being

12

248   exposed to the virus, infection was lowered to below the untreated control group (p<0.001).

249   This could not be said for the pre-treated virus, where larger dilution factors (1/1000 and

250   1/3000) did not statistically affect the degree of infection for both the $\iota-$ and λ-carrageenans.

251   Additionally, no correlation could be drawn to the extent of sulphation and its ability to

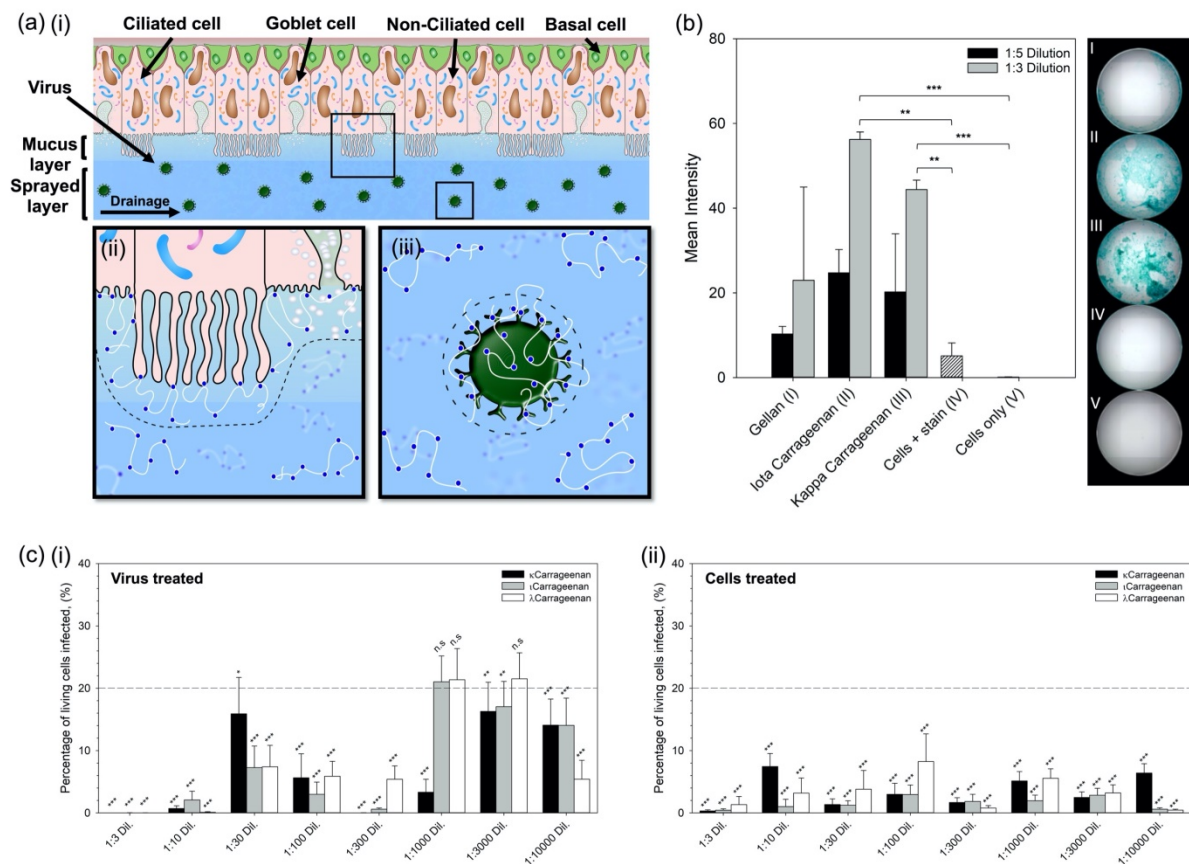252   supress infection.

253

254

255   *Figure 4: **Mechanism for the inhibition of SARS-CoV-2.** (a) schematic diagram showing the nasal epithelium covered in*

256   *the nasal spray: (i) demonstrates potential removal of the virus via trapping within the sprayed layer and elimination*

257   *through native pathways, (ii) demonstrates potential blockage of virus uptake into the cells as the polymer creates a steric*

258   *barrier across the cell interface, and (iii) demonstrates potential inhibition of virus uptake by creating a steric barrier*

259   *around the interface of the virus. (b) Alcian blue stain intensity for cells treated and subsequently washed with either gellan,*

260   *ιcarrageenan or λcarrageenan. (c) In vitro SARS-CoV-2 assay using vero cells to determine levels of infection after 48 hrs*

261   *for systems treated with increasingly sulphated carrageenans (κ<ι<λ), by either: (i) pre-treating the virus, or (ii) pre-*

262   *treating the cells. (n.s – not statistically different, * - p<0.05, ** - p<0.01, and *** - p<0.001)*

13

263 ***Discussion***

264 The role that the nasal passage plays in frontline defence, filtering harmful bacteria and

265 viruses, naturally elevates the sinonasal pathways to high risk, in terms of infection[33]. The

266 need to formulate medicines/devices which can help regulate and protect this area are thus

267 clear, however, like many regions of the body the nasal cavity poses many challenges, due to:

268 ease of access, dynamics (native clearing mechanism) and topology (inclined surfaces or

269 ceilings). As such, formulation engineering plays a decisive role in the design of novel

270 therapeutics.[34] The link between microstructure and material properties has long been

271 known, ultimately driving macroscopic responses key to both function

272 (delivery/retention/ADME – absorption, distribution, metabolism and elimination) and the

273 end user (ability to administer/patient compliance). Through a microstructural design

274 approach, the interplay between areas such as raw materials and processing can be

275 manipulated to engineer defined characteristics. In the case of a nasal spray elements such as

276 mucoadhesion, longevity, coverage and controlled delivery/prophylaxis need to be

277 considered. Polysaccharides provide perfect polymeric candidates within biological

278 applications, as the natural polymers often demonstrate biocompatibility and hold FDA

279 approval; significantly reducing risk, time and costs throughout the translational process.

280

281 A simple screening process to determine the ability to evenly spray across an inclined

282 substrate narrowed potential candidates down to both gellan gum (low acyl) and carrageenan

283 (λ). In addition to biocompatibility, their long chains (often 100s kDa) and charged side

284 groups ($-COO^-$, $-SO_3^-$) provide inherently strong mucoadhesion through polymer

285 entanglement, ionic interactions and weaker van der Waals interactions with the mucus

286 layer.[35,36] Such interactions with the mucosa provide high retention to the surface and a

14

287   mechanism of clearance, becoming transported by the cilia out of the paranasal sinuses to the

288   pharynx and eventually into the oesophagus.[29,30]

289

290   Enhancing longevity within the nasal cavity can also be sought enhanced viscosity and

291   resultant reduction in flow/clearance. The role that gellan and carrageenan play within

292   viscosity modification and related sensory attributes has been well established within the

293   food industry.[37] Again, owing to their long polymeric chains and chemistries along their

294   backbone both gellan and λcarrageenan are able to structure large volumes of water. This,

295   accompanying polymer-polymer entanglements, ultimately drives increases in viscosity,[38,39]

296   with higher polymer concentrations resulting in more viscous suspensions: until sufficiently

297   concentrated in the case of the gellan (>0.8% (w/v)), providing the evolution of a dynamic

298   yield stress. Again, yielding behaviour can be used to enhance application and slow

299   clearance, as the gravitational stress is insufficient to cause rupture of the film formed post-

300   spraying; where the film height can be estimated as a function of a typical nasal dosage (25 –

301   200 μl)[40] over a surface area *ca*. 5 cm^2.[31]

302

303   The large surface areas in the nasal cavity provides the ability to process large volumes of air

304   (up to 35 Lmin^{-1} before switching to oronasal breathing), within a total volume of *ca*. 15

305   ml.[31,40] However, the large nasal area presents a challenge to uniformly coat. Coverage of the

306   polymer systems demonstrated clear correlations between both the type of polymer and the

307   concentration of polymer used. Gellan systems demonstrated high levels of coverage across

308   all concentrations studied, suggesting an ideal candidate for nasal spray application.

309   Interestingly, λcarrageenan even though characterised by a lower viscosity, resulted in poor

310   overall coverage whilst still maintaining concentration dependency. Such changes were a

311   direct result of a shift from plume to jet formation, with gellan resulting in much faster rates

312 of jet destabilisation in comparison to the λcarrageenan. Spray behaviours comply with

313 literature, suggesting that large surface tensions as opposed to viscosity are required to force

314 droplet breakup, relative to the density of the surrounding medium.[41] As a result, the

315 persistence of a jet negatively effects patient compliance, not only providing poor coverage,

316 but eliciting unwarranted irritation on contact with the nasal wall.[42,43]

317

318 To maintain the advantage of λcarrageenan's intrinsic anti-viral capacity[44–46], formulation of

319 a composite mixture containing increasing amounts of gellan to λcarrageenan allowed for

320 optimisation of the nasal therapy. Careful control over the two polymers provided a means to

321 engineer enhanced λcarrageenan spray-ability. Interchanging 25% of the initial λcarrageenan

322 with gellan saw an increasing in the total area coated up to *ca*. 35% of its initial coverage.

323 This was further increased to *ca*. 63% on replacement of 75% of the initial polymer. In

324 addition to tailorable spray profiles, composite systems demonstrated a means to formulate

325 sprays containing λcarrageenan with both yielding and augmented viscosities, not possible

326 with the λcarrageenan alone. Data showed that the formation of intermediate products, from

327 100% λcarrageenan to 100% gellan, transitioned in behaviour governed primarily by the

328 dominating polymer. As such, it was possible to detail a set of design principles that can be

329 used to formulate various sprays, with desired mechanical properties.

330

331 Cytotoxicity and anti-viral activity of the nasal treatments were assessed using a relevant

332 enveloped virus, SARS-CoV-2, and their current gold-standard model for infection (Vero

333 cells). Initial cytotoxicity studies revealed a degree of cell death when cultured in the

334 presence of both the gellan and λcarrageenan. Such reductions in cell numbers here are

335 thought to be a consequence of osmotic stress, with high concentrations of the sugars

336 resulting in cell shock.[47] The plethora of literature demonstrating the combability and use of

16

337 such polysaccharides in pharma and biomaterials[48] might suggest that such observations are

338 indeed an artifact of two-dimensional cell culture, as opposed to inherent toxicity.

339

340 First hit and ability to prevent viral transmission was assessed using two main treatment

341 regimens. Firstly, prophylaxis was assessed through application of the spray onto the cells

342 prior to infection. Gellan systems showed limited ability to suppression the SARS-CoV-2

343 virus, whereas, λcarrageenan demonstrated complete inhibition over 48 hrs. Pre-treatment of

344 the virus, representing the ability to nullify the virus preventing transmission mirrored

345 prophylaxis data, with complete inhibition; supporting previous acknowledgements that

346 λcarrageenan provides enhanced anti-viral capacities.[49] Composites again provided the

347 ability to accommodate synergistic behaviours from both gellan and λcarrageenan: enhanced

348 mechanical responses towards spraying and anti-viral activity. Interestingly, systems

349 containing a greater proportion of gellan outperformed the λcarrageenan dominated system;

350 an unexpected outcome based on the single polymer data. Indeed, the spray was highly potent

351 with dose-dependency demonstrating significant prevention/reduction of infection up to 30-

352 and 300-fold dilutions for the virus and cell treatments, respectively.

353

354 It is suggested that inhibition of the infection results through 3 main mechanisms: formation

355 of a steric barrier at the cell interface, adsorption of the polymer to the virus, and/or physical

356 entrapment of the virus in the sprayed layer. It is proposed that polymer adsorption is

357 facilitated through charge-charge interactions at the cell and virus membrane. Although both

358 anionic in nature, the contrast in virus inhibition infers that the carrageenan's sulphate

359 chemistry drives anchoring of the polymer to the substrate surface; likely through the

360 formation of di-sulphide bridges with cationic membrane polysaccharides and/or proteins.

361 The polymer thus provides a physical role, expanding the hydrodynamic volume around the

17

362   cell/virus and preventing close proximity.[50] Even though the role that the negatively charged

363   sulphate groups play in the ability to adsorb to the bio-interface, it is unclear from the data

364   whether a link between the degree of sulphation and suppression of infection exists.

365   Although not significant in the role of coating, gellan does demonstrate its applicability when

366   considering prophylaxis through entrapment and elimination. The ability to engineer high

367   viscosities and yielding behaviour at this point becomes key, proportionally slowing

368   diffusivity, as described by the Stokes-Einstein relation.[51] To this end, diffusion of the virus

369   towards the host cells can be hampered within timescales associated with typical nasal

370   clearance.[52] In reality a combination of the 3 proposed mechanisms is likely to occur. To this

371   end, physical entrapment is suggested to provide a first means of defence, simultaneously

372   resulting in a secondary defence where cells and virus become coated. Thus, any virus

373   particles having migrated to the cell interface are already inhibited to uptake. Likewise, the

374   formation of new viruses as a result of shedding, become incapacitated. This combinatorial

375   approach, coupled with the highly potent anti-viral capacity of the carrageenan towards

376   SARS-CoV-2, provides a powerful spray device with the capacity to prevent both contraction

377   and transmission.

378   *Conclusions*

379   As the primary mode of transmission for airborne viruses is uptake through the respiratory

380   tract, the nasal passage poses one of the largest risk factors to contraction. Although it is well

381   known that the nose filters 1000s of litres of air daily, there is little in the way of preventative

382   measures to ensure protection to infection. This study has demonstrated the formulation of a

383   potent antiviral nasal spray, with not only prophylactic capacity, but the ability to prevent

384   viral transmission. Its ability to completely inhibit infection is derived from the chemistry

385   (sulphated polymer backbone) of the active polymer, λcarrageenan. Spray characteristics

386   were engineered through the production of a composite, where a set of design rules were

387   understood to allow for manipulation over the material behaviours: spray coverage, viscosity

388   and yielding behaviour. Furthermore, understanding the role of each polymer in the

389   composite allowed for a preventative mechanism, using the synergy of both material and

390   antiviral properties to coat the biological interfaces, prevent viral uptake by host cells, and

391   eliminate through native clearance pathways. As such, this work presents a potential device

392   with the capacity to specifically target infection within the nasal cavity.

393   ***Materials and methods***

394   *Materials*

395   Sodium alginate (medium viscosity), pectin from citrus peel, dextran (Mw *ca*. 20 kDa),

396   κcarrageenan,   ιcarrageenan,   λcarrageenan,   PBS,   heat   inactivated   FBS,

397   Penicillin/streptomycin, Alcian blue (8GX) were all purchased from Sigma Life Science, UK;

398   Gellan gum (CG-LA) was purchased from CP Kelco; TrypLE Express 1x was purchased

399   from Fisher Scientific; Black dye (Parker); Type 1 water (Milli-Q, Merck Millipore).

400 **Single-Component systems –** colloidal suspensions were prepared through the addition of

401 polymer (0.2 to 1.0% (w/v)) to a dilute PBS (5% v) solution. Once added, the systems were

402 vigorously mixed and left to fully hydrate for 24 hrs. All samples were kept at ambient

403 temperature (*ca.* 20 °C) until further used.

404 **Multi-Component systems –** composite mixtures were prepared by first weighing out ratios

405 of polymer (75:25, 50:50, 25:75 – gellan gum (low acyl) to λcarrageenan), and thoroughly

406 mixing. Powdered mixtures (0.2, 0.4 and 1.0% (w/v) total polymer concentration) were then

407 added to a dilute PBS (5% v) solution, vigorously mixed and left to fully hydrate for 24 hrs.

408 All samples were kept at ambient temperature (*ca.* 20 °C) until further used.

409 *Screening*

410 Polymer screening was conducted using an airbrush (750 μm aperture) coupled to an oil-free

411 compressor (Badger, US), set to 1 bar. Test material (0.9 ml) was mixed with black dye (0.1

412 ml) and sprayed across an acetate sheet set to a 45° incline. The airbrush was then cleaned

413 using a succession of 70% ethanol and water. Spray distributions were visually analysed for

414 homogeneity and retention.

415 *Rheology*

416 Viscometric analysis was undertaken on a rotational rheometer (Kinexus Ultra, Netzsch

417 Geratebeu GmbH, DE) fitted with a cone and plate (4°, 40 mm diameter) geometry. Tests

418 were conducted at 25 °C, under stress control. Dynamic viscosity was analysed by reduction

419 of the shear stress from a maximum of 100 to 0.001 Pa (dependent on test material to prevent

420 expulsion from the gap at lower viscosities) over a 2 mins ramp time. Kinexus software was

421 used to characterise the flow profiles using both power law and Cross models.

422 *Spray-ability*

423 Test material was first mixed with black dye (0.1% v) and thoroughly shaken to provide a

424 homogenous mixture. A typical handheld applicator (Adelphi, UK) was used to vertically

425 spray a paper recipient. Sprayed distributions were allowed to dry in air (no blotting effects

426 observed) and scanned at 600 DPI (greyscale). Image files were processed using an image

427 package (ImageJ), where they were initially cropped to a 2000 by 2000 px box visually

428 centred around the spray pattern. Standard thresholding was applied to all images, and scale

429 corrected equating 2000 px to 100%. Droplet analysis was conducted, and total coverage

430 determined as a percentage of the whole image. Distributions were recorded as x/y co-

431 ordinates and plotted relative to the central droplet.

432 *Infection/transmission*

433 Vero cell were washed with PBS, dislodged with 0.25% Trypsin-EDTA (Sigma life sciences)

434 and seeded into 96-well imaging plates (Greiner) at a density of 10^4 cells per well in culture

435 media (DMEM containing 10% FBS, 1% Penicillin and Streptomycin, 1% L-Glutamine and

436 1% non-essential amino acids). Cells were incubated for 24 hrs to allow time for adherence.

437 Virus or cells were treated with polymeric solutions, diluted in media, 1 hr prior to infections.

438 Cells were subsequently infected with SARS-CoV-2 virus England 2 stock 10^6 IUml^{-1} (kind

439 gift from Christine Bruce, Public health England) diluted 1/150 in culture media. Cells were

440 fixed in ice-cold MeOH after infection. Cells were then washed in PBS and stained with

441 rabbit anti-SARS-CoV-2 spike protein, subunit 1 (The Native Antigen Company), followed

442 by Alexa Fluor 555-conjugated goat anti-rabbit IgG secondary antibody (Invitrogen,

443 Thermofisher). Cell nuclei were visualised with Hoechst 33342 (Thermofisher). Cells were

444 washed with PBS and then imaged and analysed using a ThermoScientific CellInsight CX5

445 High-Content Screening (HCS) platform. Infected cells were scored by perinuclear

21

446   fluorescence above a set threshold determined by positive (untreated) and negative

447   (uninfected) controls.

448   *Cell binding*

449   **Preparation of cells –** Vero cells were expanded in T75 flasks, washed with PBS (5 ml) and

450   removed using TrypLE (2.5 ml). The cells were then re-suspended in complete media and

451   seeded in to 96 well plates (10,000 cells per well). Cells were left to attach over the

452   subsequent 24 hrs prior to treatment.

453   **Cell treatment -** cells were washed (3 times) with PBS and final washing removed. Test

454   material was diluted to either 1/3 or 1/5 and placed over the cells (200 μl) (controls were

455   treated with equal volumes of PBS). Cells were incubated for 30 minutes prior to washing (3

456   times) with PBS. Cells were subsequently stained with Alcian blue (0.1%) for 30 minutes,

457   before a final wash in PBS to remove residual stain. PBS was then added (200 μl) and wells

458   imaged.

459   **Cell Imaging –** cells were imaged using a Cytation 5M automated microplate imager. Wells

460   were images in bright field using a x4 optical lens focused on the centre of each well. Wells

461   were divided into a 6 x 4 matrix and stitched together retrospectively. Images were then

462   cropped to the well diameter using a software package (ImageJ) and colour thresholding

463   standardised and analysed for mean intensity.

464   *Statistics*

465   In all experiments data presented is an average of at least triplicates with error portrayed as

466   the 95% confidence interval. Significance was determined by first assessing data for

467   normality. Where normally distributed, paired t-tests were conducted comparing the

468   treatment group to the untreated control. If the normality test failed, comparison was made on

469   ranks using the Mann-Whitney. Significance has been shown on plots using the following

470   notation: n.s – not statistically different; * - p<0.05; ** - p<0.01; and, *** - p<0.001.

476   *References*

477   [1]   R. Dhand, J. Li, *Am. J. Respir. Crit. Care Med.* **2020**, *202*, 651.
478   [2]   R. Wathore, A. Gupta, H. Bherwani, N. Labhasetwar, *Sci. Total Environ.* **2020**, *749*,
479   141486.
480   [3]   L. Morawska, J. Cao, *Environ. Int.* **2020**, *139*, 105730.
481   [4]   V. Stadnytskyi, C. E. Bax, A. Bax, P. Anfinrud, *Proc. Natl. Acad. Sci. U. S. A.* **2020**,
482   *117*, 11875.
483   [5]   S. Kaur, H. Bherwani, S. Gulia, R. Vijay, R. Kumar, *Environ. Dev. Sustain.* **2020**, 1.
484   [6]   F. D. McCool, *Chest* **2006**, *129*, 48S.
485   [7]   S. Yang, G. W. M. Lee, C. M. Chen, C. C. Wu, K. P. Yu, *J. Aerosol Med. Depos.*
486   *Clear. Eff. Lung* **2007**, *20*, 484.
487   [8]   L. Bourouiba, *JAMA - J. Am. Med. Assoc.* **2020**, *323*, 1837.
488   [9]   T. Dbouk, D. Drikakis, *Phys. Fluids* **2020**, *32*, 053310.
489   [10]   E. Y. C. Shiu, N. H. L. Leung, B. J. Cowling, *Curr. Opin. Infect. Dis.* **2019**, *32*, 372.
490   [11]   W. F. Wells, *Am. J. Epidemiol.* **1934**, *20*, 611.
491   [12]   A. D. Langmuir, *Ann. N. Y. Acad. Sci.* **1980**, *353*, 35.
492   [13]   N. Van Doremalen, T. Bushmaker, D. H. Morris, M. G. Holbrook, A. Gamble, B. N.
493   Williamson, A. Tamin, J. L. Harcourt, N. J. Thornburg, S. I. Gerber, J. O. Lloyd-
494   Smith, E. De Wit, V. J. Munster, *N. Engl. J. Med.* **2020**, *382*, 1564.
495   [14]   F. Li, *Annu. Rev. Virol.* **2016**, *3*, 237.
496   [15]   B. G. Hogue, C. E. Machamer, in *Nidoviruses*, ASM Press, Washington, DC, USA,
497   **2014**, pp. 179–200.
498   [16]   D. Schoeman, B. C. Fielding, *Virol. J.* **2019**, *16*, 1.
499   [17]   C. M. Chan, P. C. Y. Woo, S. K. P. Lau, H. Tse, H. L. Chen, F. Li, B. J. Zheng, L.
500   Chen, J. D. Huang, K. Y. Yuen, *Exp. Biol. Med.* **2008**, *233*, 1527.
501   [18]   X. Ou, Y. Liu, X. Lei, P. Li, D. Mi, L. Ren, L. Guo, R. Guo, T. Chen, J. Hu, Z. Xiang,
502   Z. Mu, X. Chen, J. Chen, K. Hu, Q. Jin, J. Wang, Z. Qian, *Nat. Commun.* **2020**, *11*, 1.
503   [19]   J. Shang, G. Ye, K. Shi, Y. Wan, C. Luo, H. Aihara, Q. Geng, A. Auerbach, F. Li,
504   *Nature* **2020**, *581*, 221.
505   [20]   J. T. Ortega, M. L. Serrano, F. H. Pujol, H. R. Rangel, *EXCLI J.* **2020**, *19*, 410.
506   [21]   W. Sungnak, N. Huang, C. Bécavin, M. Berg, R. Queen, M. Litvinukova, C. Talavera-

López, H. Maatz, D. Reichart, F. Sampaziotis, K. B. Worlock, M. Yoshida, J. L. Barnes, N. E. Banovich, P. Barbry, A. Brazma, J. Collin, T. J. Desai, T. E. Duong, O. Eickelberg, C. Falk, M. Farzan, I. Glass, R. K. Gupta, M. Haniffa, P. Horvath, N. Hubner, D. Hung, N. Kaminski, M. Krasnow, J. A. Kropski, M. Kuhnemund, M. Lako, H. Lee, S. Leroy, S. Linnarson, J. Lundeberg, K. B. Meyer, Z. Miao, A. V. Misharin, M. C. Nawijn, M. Z. Nikolic, M. Noseda, J. Ordovas-Montanes, G. Y. Oudit, D. Pe'er, J. Powell, S. Quake, J. Rajagopal, P. R. Tata, E. L. Rawlins, A. Regev, P. A. Reyfman, O. Rozenblatt-Rosen, K. Saeb-Parsy, C. Samakovlis, H. B. Schiller, J. L. Schultze, M. A. Seibold, C. E. Seidman, J. G. Seidman, A. K. Shalek, D. Shepherd, J. Spence, A. Spira, X. Sun, S. A. Teichmann, F. J. Theis, A. M. Tsankov, L. Vallier, M. van den Berge, J. Whitsett, R. Xavier, Y. Xu, L. E. Zaragosi, D. Zerti, H. Zhang, K. Zhang, M. Rojas, F. Figueiredo, *Nat. Med.* **2020**, *26*, 681.

[22] L. Zou, F. Ruan, M. Huang, L. Liang, H. Huang, Z. Hong, J. Yu, M. Kang, Y. Song, J. Xia, Q. Guo, T. Song, J. He, H. L. Yen, M. Peiris, J. Wu, *N. Engl. J. Med.* **2020**, *382*, 1177.

[23] D. F. Proctor, *Elsevier Biomed. Press* **1982**.

[24] P. Cole, *Curr. Opin. Otolaryngol. Head Neck Surg.* **1994**, 16.

[25] P. Camner, B. Bakke, *Environ. Res.* **1980**, *21*, 394.

[26] D. Elad, M. Wolf, T. Keck, *Respir. Physiol. Neurobiol.* **2008**, *163*, 121.

[27] D. F. Proctor, *Bacteriol. Rev.* **1966**, *30*, 498.

[28] N. Mygind, R. Dahl, *Adv. Drug Deliv. Rev.* **1998**, *29*, 3.

[29] E. Houtmeyers, R. Gosselink, G. Gayan-Ramirez, M. Decramer, *Eur. Respir. J.* **1999**, *13*, 1177.

[30] N. A. Cohen, *Ann. Otol. Rhinol. Laryngol.* **2006**, *115*, 196:20.

[31] S. Gizurarson, *Curr. Drug Deliv.* **2012**, *9*, 566.

[32] Y. Liu, Z. Ning, Y. Chen, M. Guo, Y. Liu, N. K. Gali, L. Sun, Y. Duan, J. Cai, D. Westerdahl, X. Liu, K. Xu, K. fai Ho, H. Kan, Q. Fu, K. Lan, *Nature* **2020**, *582*, 557.

[33] I. Gengler, J. C. Wang, M. M. Speth, A. R. Sedaghat, *Laryngoscope Investig. Otolaryngol.* **2020**, *5*, 354.

[34] M. E. Cooke, S. W. Jones, B. ter Horst, N. Moiemen, M. Snow, G. Chouhan, L. J. Hill, M. Esmaeli, R. J. A. Moakes, J. Holton, R. Nandra, R. L. Williams, A. M. Smith, L. M. Grover, *Adv. Mater.* **2018**, DOI 10.1002/adma.201705013.

[35] S. L. Cook, S. P. Bull, L. Methven, J. K. Parker, V. V. Khutoryanskiy, *Food Hydrocoll.* **2017**, *72*, 281.

[36] N. A. Peppas, J. J. Sahlin, *Biomaterials* **1996**, *17*, 1553.

[37] A. M. Stephen, G. O. Phillips, P. A. Williams, Eds. , *Food Polysaccharides and Their Applications: Second Edition*, CRC Press, **2016**.

[38] S. Jampen, I. J. Britt, M. A. Tung, *Food Res. Int.* **2000**, *33*, 579.

[39] E. I. Yaseen, T. J. Herald, F. M. Aramouni, S. Alavi, *Food Res. Int.* **2005**, *38*, 111.

[40] P. G. Djupesland, *Drug Deliv. Transl. Res.* **2013**, *3*, 42.

[41] S. P. Lin, R. D. Reitz, *Annu. Rev. Fluid Mech.* **1998**, *30*, 85.

[42] I. Y. Z. Wong, S. E. Soh, S. Y. Chng, L. P.-C. Shek, D. Y. T. Goh, H. P. S. Van Bever, B. W. Lee, *Pediatr. Allergy Immunol.* **2010**, *21*, 1146.

[43] J. Liang, A. P. Lane, *Curr. Otorhinolaryngol. Rep.* **2013**, *1*, 51.

[44] C. B. Buck, C. D. Thompson, J. N. Roberts, M. Müller, D. R. Lowy, J. T. Schiller, *PLoS Pathog.* **2006**, *2*, 0671.

[45] A. Grassauer, R. Weinmuellner, C. Meier, A. Pretsch, E. Prieschl-Grassauer, H. Unger, *Virol. J.* **2008**, *5*, 107.

[46] Y. H. Chiu, Y. L. Chan, L. W. Tsai, T. L. Li, C. J. Wu, *Antiviral Res.* **2012**, *95*, 128.

[47] J. K. F. Wong, A. D. Metcalfe, R. K. F. Wong, J. Bush, C. Platt, *PLoS One* **2014**, *9*,

557   112672.
558 [48] L. R. Stevens, K. J. Gilmore, G. G. Wallace, M. In Het Panhuis, *Biomater. Sci.* **2016**,
559   *4*, DOI 10.1039/c6bm00322b.
560 [49] M. Baba, R. Snoeck, R. Pauwels, E. De Clercq, *Antimicrob. Agents Chemother.* **1988**,
561   *32*, 1742.
562 [50] L. B. Talarico, E. B. Damonte, *Virology* **2007**, *363*, 473.
563 [51] A. Einstein, *Ann. Phys.* **1905**, *322*, 549.
564 [52] G. M. Corbo, A. Foresi, P. Bonfitio, A. Mugnano, N. Agabitit, P. J. Colet, H. Defence,
565   *Arch. Dis. Child.* **1989**, *64*, 546.
566